Electrocatalytic Activity of Oxygen and Hydrogen Peroxide Reduction at Poly(iron tetra(o-aminophenyl) porphyrin) Coated Multiwalled Carbon Nanotube Composite Film

Yogeswaran Umasankar,* Jan-Wei Shie, and Shen-Ming Chen**,z

Department of Chemical Engineering and Biotechnology, National Taipei University of Technology, Taipei 106, Taiwan

Conductive composite film containing multiwalled carbon nanotubes (MWCNTs) coated with poly(iron tetra(o-aminophenyl) porphyrin) (PFeTAPP) has been synthesized on glassy carbon, gold, and indium tin oxide (ITO) electrodes by potentiostatic methods. The presence of MWCNTs at the electrodes enhances the surface coverage concentration (Γ) of PFeTAPP. The MWCNT-PFeTAPP composite film produced on gold electrode has been used for electrochemical quartz crystal microbalance studies, which reveal enhancements in the functional properties of composite film due to the presence of both the MWCNTs and PFeTAPP. The surface morphology of the composite film deposited on an ITO electrode has been studied using scanning electron microscopy and atomic force microscopy. These studies reveal that there is an incorporation of PFeTAPP with MWCNTs. The MWCNT-PFeTAPP composite film exhibits promising electrocatalytic activity toward the reduction of O_2 and H_2O_2, which has been studied using cyclic voltammetry. Further, O_2 reduction has been enhanced at the composite film with the help of myoglobin as a mediator. The MWCNT-PFeTAPP film's sensitivity values are higher than the values obtained for PFeTAPP and MWCNT films separately. Finally, *I-t* curve study has been conducted for the amperometric detection of H_2O_2 at the MWCNT-PFeTAPP composite film. The amperometric results show higher sensitivity values than the results obtained with the voltammetric technique.
© 2009 The Electrochemical Society. [DOI: 10.1149/1.3232005] All rights reserved.

The surface modification of electrodes with carbon nanotubes (CNTs) has led to recent developments in the electrocatalysis field. Among such developments, the detection of bio-organic and inorganic compounds at the CNT matrices have been widely reported.[1-4] The rolled-up graphene sheets of carbon, i.e., CNTs, exhibit a π-conjugative structure with a highly hydrophobic surface. This property of CNTs allows them to interact with various compounds through π-π electronic and hydrophobic interactions.[5-7] These interactions are used for preparing sandwiched film-modified electrodes for electrocatalytic studies.[8,9] Similarly, electropolymerization is a simple but powerful method in targeting selective modification of different types of electrodes with desired matrices. Numerous conjugated polymers have been electrochemically synthesized for their application in the fabrication of chemical and biochemical sensor devices.[10] These conjugated polymers for sensor devices have exhibited an interesting enhancement in the electrocatalytic activity toward the oxidation or reduction of several biochemical and inorganic compounds[11] where some of the functional groups in the polymers act as catalysts.[12-14] Even though the electrocatalytic activities of CNT and conjugated polymer films are good individually, some properties such as mechanical stability, sensitivity for different techniques, and electrocatalytic activity for multiple compounds are not efficient. So, studies were developed in the past decade for the preparation of composite films.[15] These composite films are composed of both CNTs and electroactive polymers to enhance the electrocatalytic activity.[16-21] Electrodes modified with composite films have been widely used in capacitors, battery, material science, photoelectrochemistry, fuel cells, chemical sensors, and biosensors.[22-24]

Among the above-mentioned electroactive polymers, few porphyrin- and metalloporphyrin-based polymers are of considerable interest for the development of sensor devices.[25,26] Various metalloporphyrin monomers have also been employed as the electroactive membrane component of chloride-selective electrodes.[27-32] Similarly, the electrocatalytic reduction of oxygen and hydrogen peroxide at porphyrin-modified electrodes was reported in Ref. 33 and 34. H_2O_2 is the most valuable marker of oxidative stress.[35,36] H_2O_2 is also present in underground water and rainwater, which resulted from industries and atomic power stations. These factors increase the necessity for the quantitative measurement of H_2O_2.[37,38]

As a consequence, its reduction and accurate determination at low potential constitute a valuable task and search for sensitive and selective methods. Other major applications for the reduction of O_2 and H_2O_2 are fuel cells. Not only limited to these analytes, other analytes such as organohalides were also studied using iron-porphyrin-modified electrodes.[39]

The literature survey reveals no previous attempts made for the synthesis of composite films composed of CNTs and poly(metalloporphyrin) for sensor applications. Generally, porphyrins have a rich redox chemistry and can bind many analytes above and below the porphyrin ring plane as axial ligands, which makes them suitable for the composite film preparation. In this paper, we report on a composite film made of multiwalled carbon nanotubes (MWCNTs) incorporated with poly(iron tetra(o-aminophenyl) porphyrin) (PFeTAPP). A detailed characterization of the MWCNT-PFeTAPP composite film, along with its enhancement in functional properties, peak current, and electrocatalytic activity toward O_2 and H_2O_2, is also reported in this paper. The MWCNT-PFeTAPP composite film has been formed on a glassy carbon electrode (GCE) by uniformly coating and drying well-dispersed MWCNTs and then by the electropolymerization of iron tetra(o-aminophenyl) porphyrin (FeTAPP) on the MWCNT-modified GCE from acidic aqueous solution.

Experimental

Materials.— FeTAPP, MWCNTs (outside diameter of 10–20 nm, inside diameter of 2–10 nm, and length of 0.5–200 μm), potassium, and H_2O_2 obtained from Aldrich and Sigma-Aldrich and were used as received. All other chemicals used were of analytical grade. The preparation of aqueous solution was done twice with distilled deionized water. Solutions were deoxygenated by purging with prepurified nitrogen gas. The pH 1.5 aqueous solution was prepared from 0.1 M Na_2SO_4, where the pH was adjusted using H_2SO_4.

Apparatus.— Cyclic voltammetry (CV) and rotating ring disk electrode (RRDE) were performed using analytical system models CHI-611, CHI-400, and CHI-750 potentiostats. A conventional three-electrode cell assembly consisting of Ag/AgCl reference electrode (the activity of the chloride ions was 3.5 mol kg^{-1}) and a Pt wire counter electrode were used for the electrochemical measurements. The working electrode was either an unmodified GCE or GCE modified with PFeTAPP, MWCNTs, or MWCNT-PFeTAPP composite films. In these experiments, all the potentials were reported vs the Ag/AgCl reference electrode. The working electrode for electrochemical quartz crystal microbalance (EQCM) measure-

* Electrochemical Society Student Member.
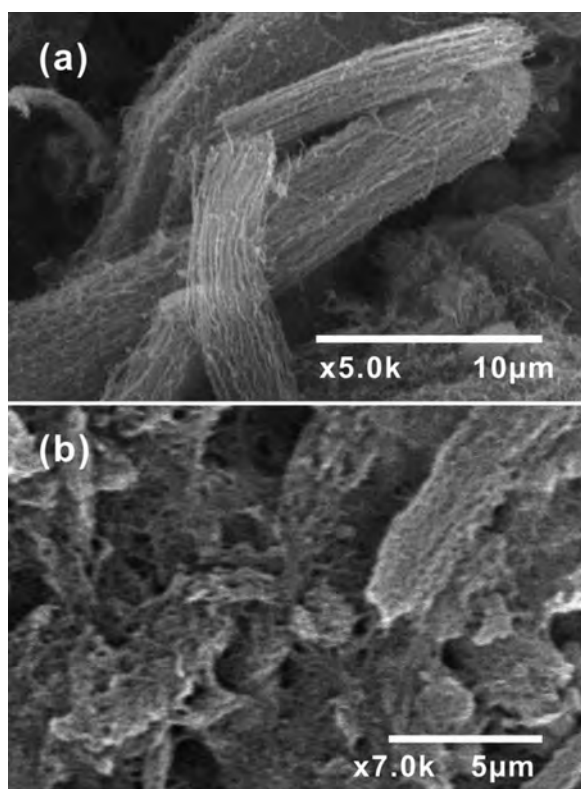** Electrochemical Society Active Member.
z E-mail: smchen78@ms15.hinet.net

Figure 1. SEM images of (a) unprocessed MWCNTs and (b) functionalized MWCNTs.

ment was an 8 MHz AT-cut quartz crystal coated with gold. The diameter of the quartz crystal was 13.7 mm; the gold electrode diameter was 5 mm. The morphological characterizations of the films were examined by scanning electron microscopy (SEM) (Hitachi S-3000H) and atomic force microscopy (AFM) (Being Nano-Instruments CSPM4000). All the measurements were carried out at $25 \pm 2°C$.

Preparation of MWCNT dispersion and MWCNT-PFeTAPP composite electrode.— There was an important challenge in the preparation of MWCNT dispersion. Because of its hydrophobic nature, it was difficult to disperse them in any aqueous solution to get a homogeneous mixture. Briefly, the hydrophobic nature of MWCNTs was converted into a hydrophilic nature by following previous studies.[3,15,40] This was done by weighing 10 mg of MWCNTs and 200 mg of potassium hydroxide into a ruby mortar and by graining them together for 2 h at room temperature. Then, the reaction mixture was dissolved in 10 mL of double-distilled deionized water and precipitated many times into methanol for the removal of potassium hydroxide. Then, the MWCNTs obtained in 10 mL water were ultrasonicated for 6 h to get a uniform dispersion. This functionalization process of MWCNTs was to obtain a hydrophilic nature for the homogeneous dispersion in water. This process not only converted the MWCNTs into a hydrophilic nature but also helped to break down larger bundles of the MWCNTs into smaller ones. This result was confirmed using SEM, as shown in Fig. 1, where (a) is the unprocessed MWCNTs and (b) is the functionalized MWCNTs.

Before starting each experiment, the GCEs were polished by a bioanalytical systems (BAS) polishing kit with 0.05 μm alumina slurry, then rinsed and ultrasonicated in double-distilled deionized water. The GCEs studied were uniformly coated with 51, 77, and 103 μg cm^{-2} of MWCNTs and dried at room temperature. Then, FeTAPP (0.1 mM) was electropolymerized on the MWCNT-modified GCE, which was present in pH 1.5 aqueous solution. The electropolymerization was performed by consecutive cyclic voltam-

mograms over a suitable potential range of −0.3 to 1.0 V. Then, the modified MWCNT-PFeTAPP electrode was carefully washed with double-distilled deionized water. The concentrations of homogeneously dispersed MWCNTs were exactly measured using a microsyringe.

Results and Discussion

Synthesis and CV studies of various composite films composed of PFeTAPP and MWCNTs.— The electropolymerization of FeTAPP (0.1 mM) using electrochemical oxidation on the MWCNT-modified and MWCNT-unmodified GCEs has been performed for the preparation of the MWCNT-PFeTAPP composite film and PFeTAPP film, respectively (figures not shown). Four redox couples have been obtained for PFeTAPP on the MWCNT-modified and MWCNT-unmodified GCEs. For both films, the $E^{0'}$ values of four redox couples are 660.7, 516.6, 322.2, and −49.25 mV vs Ag/AgCl in pH 1.5 aqueous solution. Among these four redox couples, $E^{0'}$ at −49.25 mV represents the Fe$^{III/II}$ redox reaction of FeTAPP, and the other redox couples represent the ring of FeTAPP.[41] In these experiments, MWCNT-modified GCE shows higher polymerizing current for PFeTAPP than at bare GCE, which represents more deposition of PFeTAPP on MWCNT-modified GCE. The effect of various concentrations of MWCNTs toward FeTAPP electropolymerization has been studied, as shown in Fig. 2a. These cyclic voltammograms in Fig. 2a (composites 1, 2, and 3) represent 51, 77, and 103 μg cm^{-2} loadings of MWCNTs present in the MWCNT-PFeTAPP film on GCE, respectively. Obviously, the peak currents of the PFeTAPP increases when increasing the load of the MWCNTs on GCE. Among all these four films, the peak currents of redox couples are predominant only for the composite 3 film. Based on the above result, for other electrochemical studies, composite 1 and 2 films have been excluded. Similar to the GCE, gold electrodes have also been used to characterize the composite 3 films in pH 1.5 aqueous solution. Figure 2b represents the redox peaks of PFeTAPP and composite 3 films at gold electrode, which shows that composite 3 has higher peak currents than PFeTAPP. This result also reveals the importance of the presence of MWCNTs in the composite film, where MWCNTs enhance the electron transfer on various electrodes, which in turn widen the sensor-based applications.

EQCM studies of PFeTAPP formation on MWCNT-modified and MWCNT-unmodified electrodes.— The EQCM experiments have been carried out by modifying the gold present on the electrochemical quartz crystal with uniformly coated MWCNTs. After modifying, the crystals have been dried at 35°C. The EQCM result also shows that the obvious deposition potential started between −0.3 and 1.0 V (figure not shown). From the frequency change, the change in the mass of composite film at quartz crystal has been calculated using the Sauerbrey equation; however a 1 Hz frequency change is equivalent to 1.4 ng of mass change.[8,42,43] The mass changes during the PFeTAPP deposition on the MWCNT-modified gold and bare gold electrodes for total cycles are calculated, and they are 40 and 24 ng cm^{-2}, respectively. However, in both cases, because of the poor electron transfer, the redox peak currents are low (not shown in figure). Figure 2c indicates the gross frequency change with the increase in scan cycles, and Fig. 2d indicates each consecutive cycle frequency change with the increase in scan cycles. From Fig. 2c, clearly, there has been an increase in the deposition rate of PFeTAPP on MWCNT-modified gold than on bare gold. Similarly, Fig. 2d shows a decrease in the rate of PFeTAPP deposition on bare gold in each consecutive cycle, whereas the deposition on MWCNT-modified gold increases constantly after the second cycle. This proves that the deposition of PFeTAPP on the MWCNT film is more stabilized and more homogeneous than that on the bare electrode. Similar previous studies on the CNT composite also show the necessity of the CNTs for improving the functional properties such as orientation, enhanced electron transport, and high capacitance.[44,45]
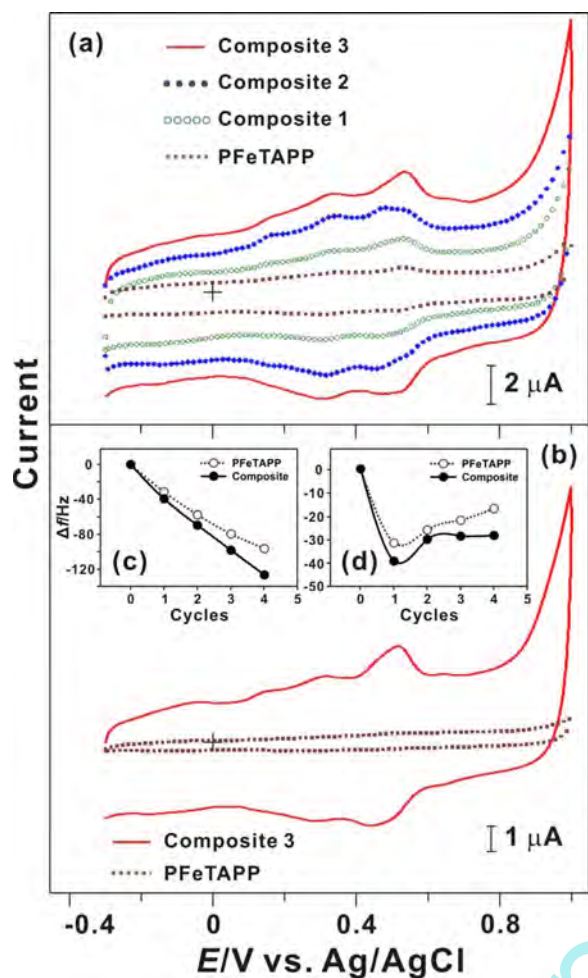
Figure 2. (Color online) (a) Cyclic voltammograms of GCE modified from PFeTAPP; composite 1, 2, and 3 films in pH 1.5 aqueous solution; and scan rate at 20 mV s^{-1}, where 1, 2, and 3 represent 51, 77, and 103 μg cm^{-2} of MWCNTs in the composite film, respectively. Similarly, (b) represents the cyclic voltammograms of gold electrode modified from PFeTAPP and composite 3 at similar conditions to that of GCE. The EQCM frequency change responses recorded together with the consecutive cyclic voltammograms (PFeTAPP formation on MWCNT-modified and MWCNT-unmodified electrodes, potential values between −0.3 and 1.0 V, and scan rate at 20 mV s^{-1}), where (c) shows the gross change in the frequency shift for the four-scan cycles, whereas (d) shows the change between each consecutive scan.

Electrochemical characterizations of Fe$^{III/II}$ redox reaction at various composite films composed of PFeTAPP and MWCNTs.— Detailed electrochemical characterizations of the Fe$^{III/II}$ redox reaction at PFeTAPP have been investigated using CV studies. Similar to the earlier part of the Results and Discussion section, various loadings of the MWCNT composites along with PFeTAPP (four different films) have been prepared and studied in pH 1.5 aqueous solution, as shown in Fig. 3a. To obtain only the Fe$^{III/II}$ redox couple, the potential range for the above-mentioned CV studies has been limited from −0.3 to −0.15 V. Among all these four films, the redox peak at $E^{0'} = -49.25$ mV (Fe$^{III/II}$) is predominant only for the composite 3 film. This increase in the peak current (at $E^{0'} = -49.25$ mV) for composite 3 and the surface coverage (Γ) concentration values for the same catalyst given in Table I are similar. Assuming that one electron transfer is involved for PFeTAPP (Fe$^{III/II}$ species) in pH 1.5, the Γ values have been calculated by using the equation $\Gamma = Q/nFA$, where Q is the charge involved in the reaction, n is the number of electron transferred, F is Faraday's
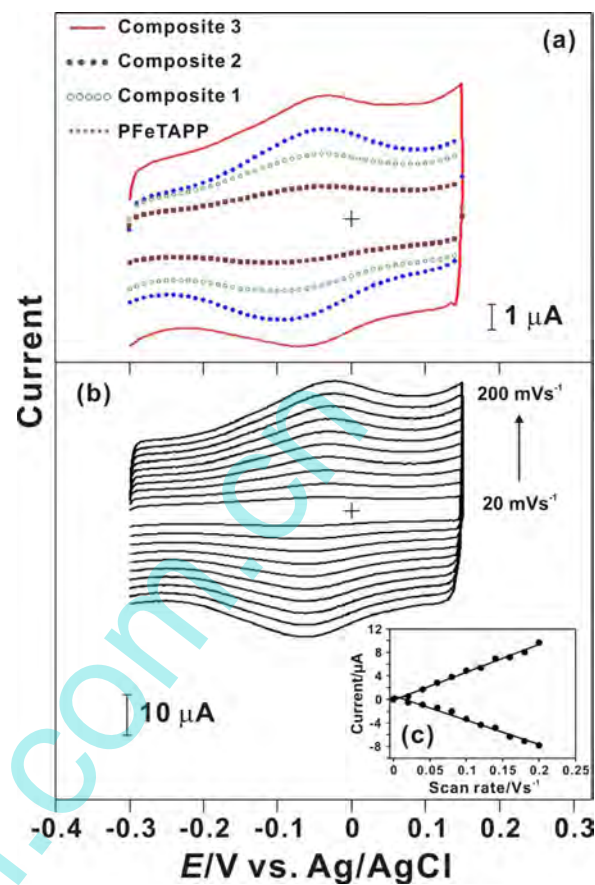

Figure 3. (Color online) (a) CV studies of the redox peak current at $E^{0'}$ = −52.35 mV of GCE modified from PFeTAPP; composite 1, 2, and 3 films in pH 1.5 aqueous solution; and scan rate at 20 mV s^{-1}. (b) Cyclic voltammograms of composite 3 film in pH 1.5 aqueous solution: scan rate at 20–200 mV s^{-1} with the increment of 20 mV s^{-1} for each cycle. (c) The plot of redox peak currents ($E^{0'}$ = −52.35 mV) of composite 3 film vs scan rate from 20 to 200 mV s^{-1} in pH 1.5 aqueous solution.

constant, and A is the electrode area.[41] These results indicate that the concentration increase of the MWCNTs increases the Γ of PFeTAPP (Fe$^{III/II}$ species). The Γ increase can be explained as the concentration of the MWCNTs directly proportional to the geometric area, where the MWCNT-modified GCE contains more surfaces to hold PFeTAPP compared to the bare GCE surface. The geometric area of nanomaterials is higher than the bulk materials. This result is similar to the EQCM result, where the presence of MWCNTs enhances the deposition of PFeTAPP. The slope value obtained from Table I reveals that the increase in Γ of PFeTAPP per microgram of MWCNTs is ≈3 pmol cm^{-2} μg^{-1}.

The cyclic voltammograms of the composite 3 film on GCE in pH 1.5 aqueous solution at different scan rates have been studied, as

Table I. Surface coverage concentrations (Γ) of Fe$^{III/II}$ species present in PFeTAPP at different types of modified electrodes obtained using CV in pH 1.5 aqueous solution.

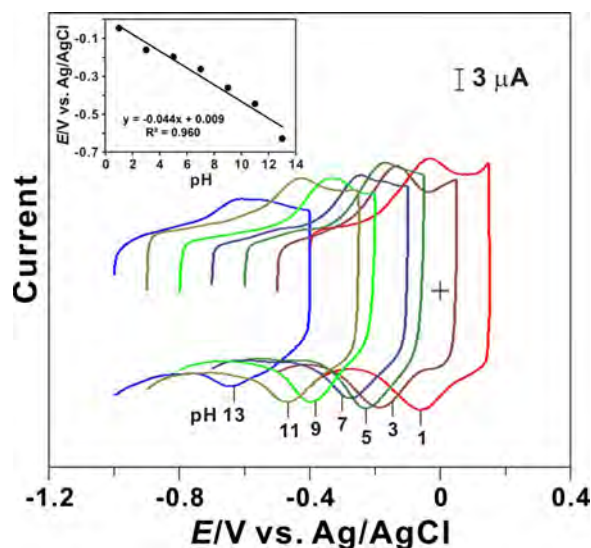| Electrode type	Modified film	Γ (pmol cm^{-2})
GCE	PFeTAPP	65.3
	Composite 1	202.6
	Composite 2	337.8
	Composite 3	456.7

Figure 4. (Color online) Cyclic voltammograms of the composite 3 film synthesized using pH 1.5 aqueous solution on GCE and transferred to various pH solutions. The insets show the formal potential vs pH from 1 to 13 (slope = −44 mV/pH), where the slope is almost nearer to the Nernstian equation for nonequal numbers of electrons and protons transfer.

Figure 5. SEM images of (a) PFeTAPP and (b) MWCNT-PFeTAPP composite films.

shown in Fig. 3b, which shows the anodic and cathodic peak currents of the $Fe^{III/II}$ species in the composite 3 film. The redox peak intensity linearly increases with the increase in scan rates up to 200 mV s^{-1}. The inset graph in Fig. 3c shows that the ratio of I_{pa}/I_{pc} remained almost in unity, as expected for the surface-type behavior. The above results demonstrate that the redox process has not been controlled by diffusion up to 200 mV s^{-1}. Figure 4 shows the cyclic voltammograms of composite 3 film present on GCE prepared using pH 1.5 aqueous solution, then washed with deionized water, and measured in various pH aqueous solutions (in the absence of FeTAPP). These cyclic voltammograms show that the film is highly stable in the pH range between 1 and 13. The values of E_{pa} and E_{pc} depend on the pH value of the buffer solution. The inset in Fig. 4 shows the change in the formal potential of composite 3 ($Fe^{III/II}$ species) plotted over the pH range of 1–13. The response shows a slope of −44 mV pH^{-1}, which is close to that given by the Nernstian equation for nonequal numbers of electrons and proton transfer.[46,47] The above results show that the presence of both the MWCNTs and PFeTAPP enhances the electrochemical properties of composite 3 in a wide range of pH solutions.

Morphological studies of MWCNT, PFeTAPP, and MWCNT-PFeTAPP films.— Three different films [MWCNT (Fig. 1b), PFeTAPP (Fig. 5a), and MWCNT-PFeTAPP (Fig. 5b)] have been prepared on indium tin oxide (ITO) electrodes with similar conditions and similar potential values as those of GCE and were characterized using SEM. From Fig. 1b to Fig. 5, it is significant that there are morphological differences between all these three films. The morphological structure in Fig. 5a shows the formation of beads of PFeTAPP on ITO. Similarly, in Fig. 5b, the deposition of PFeTAPP on MWCNTs forms a composite film, where PFeTAPP completely covers the MWCNTs. The morphology of the MWCNTs in Fig. 5b is not visible, as shown in Fig. 1a, because of the deposition of PFeTAPP on MWCNTs. The same modified ITO electrodes have been used to measure the AFM topography images, and these measured morphological structures are similar to that of SEM. Figure 6b shows the beads of PFeTAPP, whereas in Fig. 6c, the MWCNTs are covered by PFeTAPP. Figure 6a shows the presence of MWCNTs on ITO. When comparing all these three AFM images, the thickness of the MWCNT-PFeTAPP composite film is higher than the other two
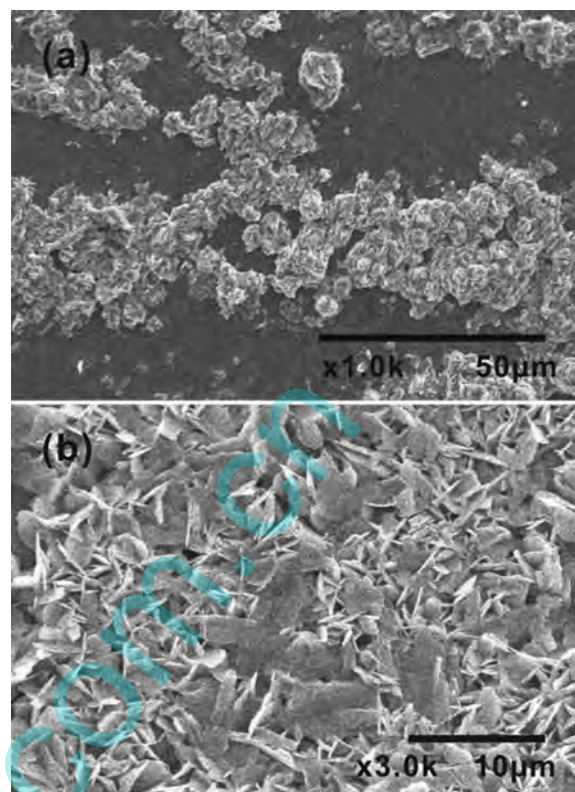
films. These SEM and AFM results reveal the presence of both PFeTAPP and MWCNT in the MWCNT-PFeTAPP composite film.

Mediated oxygen reduction at PFeTAPP, MWCNT, and composite 3 films.— The reduction of O_2 at three different modified GCEs (PFeTAPP, MWCNTs, and composite 3) in the presence and in the absence of 10 μM myoglobin (MB) has been studied, as shown in Fig. 7. The MB catalyst has been added to the electrolyte for the required experiments. The electrolyte used for all these experiments was an aqueous solution of 0.1 M Na_2SO_4, where pH is adjusted to 1.5 using H_2SO_4. The scan rate of the cyclic voltammograms in Fig. 7 is 20 mV s^{-1}. For comparison, studies of the same experiments have also been carried out with O_2 and without O_2 using nitrogen purging. The dotted lines in all these figures show the reduction of O_2 at bare GCE. Initially, bare GCE has been used to study the O_2 reduction at three different conditions as follows: N_2 saturated with 10 μM MB, O_2 saturated without MB, and O_2 saturated with 10 μM MB. These results at bare GCE show that the presence of MB in the electrolyte enhances the electrocatalytic activity of O_2 reduction. In this, the word "enhanced electrocatalysis" could be explained as either an increase in peak current or a lower overpotential or both.[48] This enhancement of the electrocatalytic activity in the presence of MB is due to the homogeneous mediation by MB, which is similar to the hemoglobin in a previous report.[41]

Following the studies at bare GCE, the MB-catalyzed O_2 reduction has also been studied at the PFeTAPP, MWCNT, and composite 3 films, as shown in Fig. 7a-c, respectively. Similarly, the experimental conditions for these three modified electrodes are N_2 saturated without MB, N_2 saturated with 10 μM MB, O_2 saturated without MB, and O_2 saturated with 10 μM MB. The E_{pc} and I_{pc} values of all these experimental results are given in Table II. These results also show that the presence of MB in the electrolyte enhances the electrocatalytic activity of O_2 reduction at different modified electrodes. A detailed investigation of all these CV results shows that the composite 3 has three different reduction peaks for
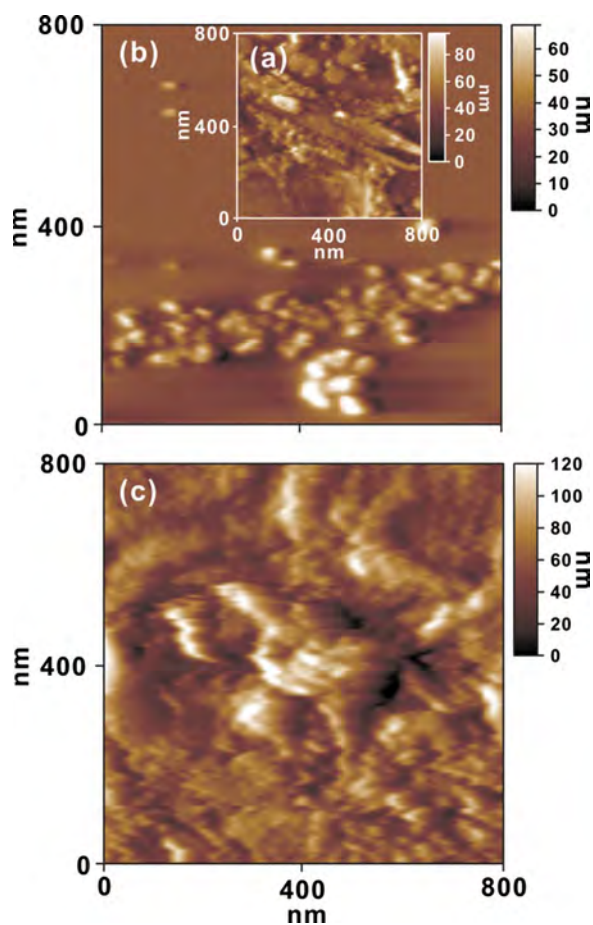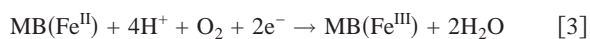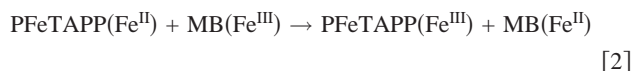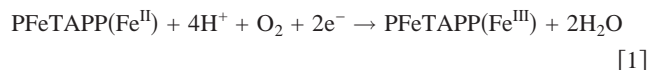
Figure 6. (Color online) AFM images of (a) MWCNT, (b) PFeTAPP, and (c) MWCNT-PFeTAPP composite films.
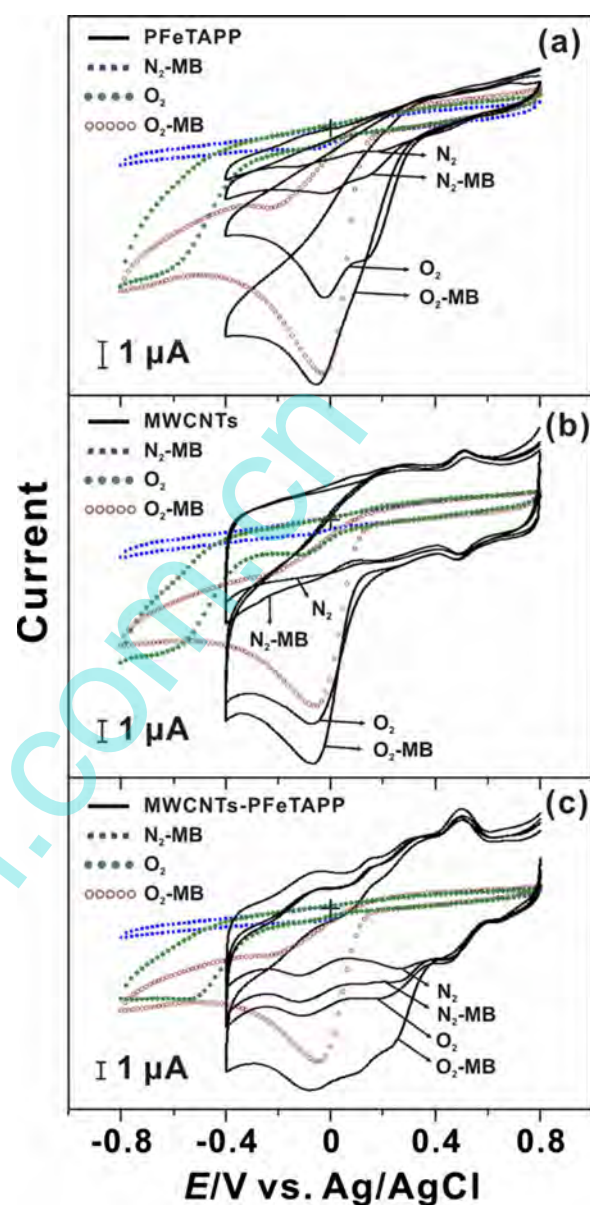

Figure 7. (Color online) Cyclic voltammograms of (a) PFeTAPP, (b) MWCNT, and (c) composite 3 film modified the GCEs using pH 1.5 aqueous solution under the following experimental conditions: N_2 saturated without MB, N_2 saturated with 10 μM MB, O_2 saturated without MB, and O_2 saturated with 10 μM MB. In all sections, the noncontinuous lines (dotted, squared, and frame circled) represent bare GCE at similar experimental conditions.

O_2, which are absent from the other films (Table II). Especially, when comparing all the other films, the peak at $E_{pc} = 214$ mV for O_2 in the presence of MB at the composite 3 electrode shows both lower overpotential and increased peak current. This decrease in overpotential arises because of the presence of PFeTAPP in the composite 3 film. Similarly, the increase in peak current arises because of the presence of both MWCNTs and MB. The comparison of the composite 3 film and the previously reported result in Ref. 41 (E_{pc} and I_{pc} values) shows that the composite 3 possesses enhanced electrocatalysis toward the O_2 reduction in the presence of MB. The electrochemical reduction of O_2 to H_2O at the MWCNT-PFeTAPP film in the presence of MB could be given by the following equations

$$PFeTAPP(Fe^{II}) + 4H^+ + O_2 + 2e^- \rightarrow PFeTAPP(Fe^{III}) + 2H_2O$$
$$[1]$$

$$PFeTAPP(Fe^{II}) + MB(Fe^{III}) \rightarrow PFeTAPP(Fe^{III}) + MB(Fe^{II})$$
$$[2]$$

$$MB(Fe^{II}) + 4H^+ + O_2 + 2e^- \rightarrow MB(Fe^{III}) + 2H_2O \qquad [3]$$

Further investigation of O_2 reduction in the presence of MB by composite 3 has been done using RRDE. Figure 8 shows the electrochemical reduction of O_2 by a composite 3 film-modified GC disk electrode (at 0.1 and 0.2 V) and the electrochemical oxidation of H_2O_2 by a bare platinum ring electrode (at 0.8 V) in pH 1.5 aqueous solution. The increase in the concentration of O_2 increases the disk current (I_D). However, the platinum ring current (I_R) does not show

an increase in current during the increase in O_2 concentration, which shows that there is no formation of H_2O_2 during O_2 reduction at the disk electrode.

Electrocatalytic activity of H_2O_2 reduction at PFeTAPP, MWCNT, and composite 3 films.— Figure 9a shows the electrocatalytic reduction of H_2O_2 using CV. The electrolyte used for the electrocatalytic reduction reaction was an aqueous solution of 0.1 M Na_2SO_4, where pH is adjusted to 1.5 using H_2SO_4. Before the start of each CV recording, the electrolyte has been purged with nitrogen for 10 min. The scan rate used for these electrocatalysis experiments was 20 mV s^{-1}. Four modified electrodes (bare GCE, PFeTAPP, MWCNT, and composite 3 films) have been investigated for electrocatalytic activity. The cyclic voltammograms of the composite 3 film in Fig. 9a exhibit a reversible redox couple for PFeTAPP

Table II. Comparison of E_{pc} and I_{pc} values of the mediated O_2 reduction at different modified GCEs in the presence (O) and in the absence (X) of O_2 and MB in pH 1.5 aqueous solution.

Modified GCEs	O_2	MB	E_{pc} (mV)	I_{pc} (nA)
Bare GCE	X	O	−69	−463
	O	X	−91, −706	−271.5, −3595
	O	O	−22	−9041
PFeTAPP	X	X	205, −116	−85.27, −51.73
	X	O	136, −7	−705.4, −222.7
	O	X	125, −17	−4077, −1085
	O	O	−49	−8577
MWCNT	X	X	−27	−782.1
	X	O	−4	−501.3
	O	X	−61	−5952
	O	O	−62	−8829
Composite 3	X	X	256, −130	−553, −1103
	X	O	231, −127	−1498, −1146
	O	X	175, −107	−2265, −1096
	O	O	214, 102, −84	−4672, −527.2, −1688

($Fe^{III/II}$) in the absence of analytes; upon the addition of analytes, a growth in the reduction peak of H_2O_2 appeared at $E_{pc} = -0.16$ V. This peak potential shows that the electrocatalytic reduction of H_2O_2 has taken place at PFeTAPP (Fe^{II}) and could be represented by the following equation

$$FeTAPP(Fe^{II}) + H_2O_2 + 2H^+ + 2e^- \rightarrow FeTAPP(Fe^{III}) + 2H_2O$$

[4]
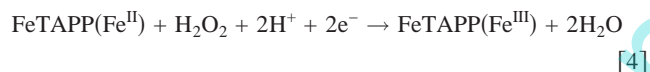
During the electrocatalysis experiments, an increase in the concentration of the analyte simultaneously produced a linear increase in the reduction peak current of the analyte, as shown in the inset of Fig. 9a. Composite 3 shows a higher peak current for H_2O_2 when compared to the PFeTAPP, MWCNT-modified, and MWCNT-unmodified GCEs. The values of I_{pc} and E_{pc} for H_2O_2 at different films are given in Table III. From the slopes of linear calibration
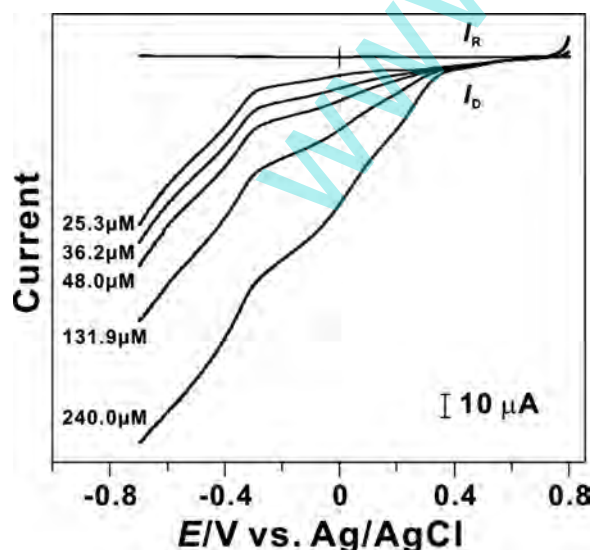

Figure 8. RRDE voltammograms of composite 3 film (at 1600 rpm) in pH 1.5 aqueous solution with various concentrations of $O_2 = 25.3–240$ μM; scan rate at 15 mV s^{-1}, where I_D and I_R are GC disk electrode and platinum ring electrode currents ($E_R = 0.8$ V vs Ag/AgCl), respectively.
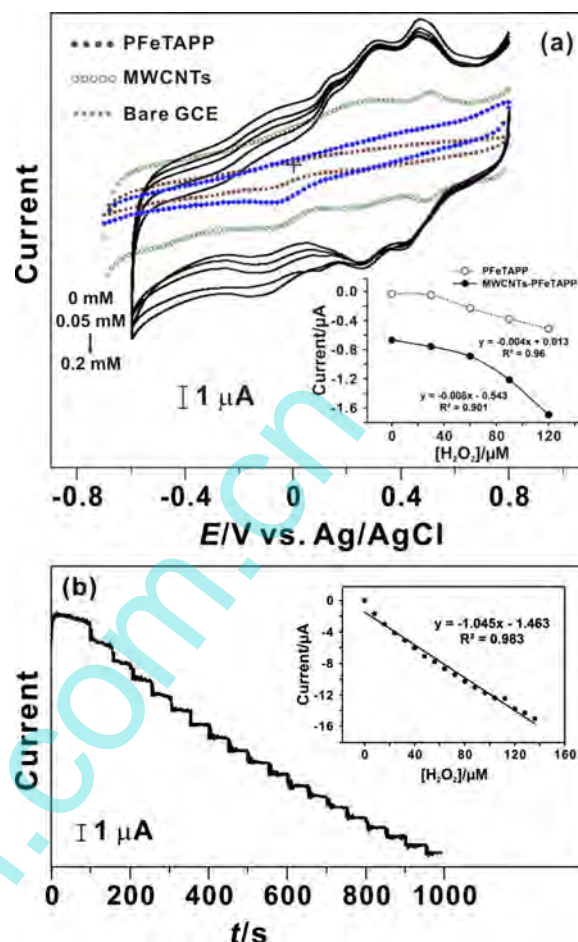

Figure 9. (Color online) (a) Cyclic voltammograms of composite 3 film (continuous dark lines) in pH 1.5 aqueous solution with various concentrations of H_2O_2 (0.0, 0.05, 0.1, 1.15, and 0.2 mM). The inset in (a) shows the plot of CV peak current vs different concentrations of H_2O_2 at PFeTAPP and composite 3 films. (b) I-t curve is a result of composite 3 film in pH 1.5 aqueous solution (at 1200 rpm and potential = −0.16 V) in the presence of H_2O_2 from 0, 8.0 to 136 μM. The inset in (b) shows the plot of current vs different concentrations of H_2O_2 obtained using I-t curve for composite 3 film.

curves, the sensitivity of PFeTAPP and composite 3 modified GCEs and their correlation coefficient have been calculated and given in Table IV. Clearly, the sensitivity of composite 3 is higher for H_2O_2 than at PFeTAPP. Figure 9b is the amperometric response of the composite 3 film with successive addition of H_2O_2 in the concentration ranging from 8.0 to 136 μM at the potential of −0.16 V. In these results, the amperometric response reaches about 5 s upon the addition of H_2O_2, and the response is proportional to its concentration. The sensitivity value for the H_2O_2 reduction at composite 3 in

Table III. Comparison of E_{pc} and I_{pc} values of the H_2O_2 reduction at different modified GCEs in pH 1.5 aqueous solution.

Modified GCEs	E_{pc} (mV)	I_{pc} (nA)
Bare GCE	−104	−469.5
PFeTAPP	−48	−560.8
MWCNT	−117	−949.8
Composite 3	−164	−1652

Table IV. Sensitivity and correlation coefficient of different modified electrodes for H₂O₂ obtained using voltammetric and amperometric techniques in pH 1.5 aqueous solution.

Modified GCEs	Techniques	Sensitivity ($\mu A\ \mu M^{-1}\ cm^{-2}$)	Correlation coefficient of the slope
PFeTAPP	CV	−0.05	0.960
Composite 3	CV	−0.10	0.901
	I-t curve	−6.53	0.983

the amperometric technique is higher than the value obtained in CV (Table IV). These results show that the composite 3 film can be efficiently used for H_2O_2 detection.

Conclusions

We have developed a composite material composed of MWCNTs and PFeTAPP at GCE, gold, and ITO electrodes, which are more stable in pH 1.5 aqueous solution. The MWCNT-PFeTAPP composite film used for the electrocatalysis combines the advantages of ease of fabrication, high reproducibility, and sufficient long-term stability. The EQCM results confirm the incorporation of PFeTAPP on an MWCNT-modified gold electrode. The SEM and AFM results show the differences between PFeTAPP, MWCNT, and MWCNT-PFeTAPP composite films. Further, the MWCNT-PFeTAPP composite film has excellent functional properties with good electrocatalytic activity on compounds such as O_2 (in the presence of MB) and H_2O_2. The experimental methods of the CV and *I-t* curve with a composite film biosensor integrated into the GCE presented in this paper provide an opportunity for qualitative and quantitative characterizations. Therefore, this work establishes and illustrates, in principle and potential, a simple approach for the development of voltammetric and amperometric sensors based on the MWCNT-PFeTAPP composite-modified glassy carbon, gold, and ITO electrodes.

Acknowledgments

References

1. G. Wu, Y. S. Chen, and B. Q. Xu, *Electrochem. Commun.*, **7**, 1237 (2005).
2. J. S. Ye, Y. Wen, W. D. Zhang, H. F. Cui, G. Q. Xu, and F. S. Sheu, *Nanotechnology*, **17**, 3994 (2006).
3. U. Yogeswaran and S. M. Chen, *Electrochim. Acta*, **52**, 5985 (2007).
4. J. Wang, M. Li, Z. Shi, N. Li, and Z. Gu, *Electrochim. Acta*, **47**, 651 (2001).
5. Q. Li, J. Zhang, H. Yan, M. He, and Z. Liu, *Carbon*, **42**, 287 (2004).
6. J. Zhang, J. K. Lee, Y. Wu, and R. W. Murray, *Nano Lett.*, **3**, 403 (2003).
7. A. Star, T. R. Han, J. Christophe, P. Gabriel, K. Bradley, and G. Gruner, *Nano Lett.*, **3**, 1421 (2003).
8. M. Zhang, K. Gong, H. Zhang, and L. Mao, *Biosens. Bioelectron.*, **20**, 1270 (2005).
9. R. J. Chen, Y. Zhang, D. Wang, and H. Dai, *J. Am. Chem. Soc.*, **123**, 3838 (2001).
10. C. P. McMahon, G. Rocchitta, S. M. Kirwan, S. J. Killoran, P. A. Serra, J. P. Lowry, and R. D. O'Neill, *Biosens. Bioelectron.*, **22**, 1466 (2007).
11. I. Becerik and F. Kadirgan, *Synth. Met.*, **124**, 379 (2001).
12. T. Selvaraju and R. R. Ramaraj, *J. Electroanal. Chem.*, **585**, 290 (2005).
13. M. Mao, D. Zhang, T. Sotomura, K. Nakatsu, N. Koshiba, and T. Ohsaka, *Electrochim. Acta*, **48**, 1015 (2003).
14. M. Yasuzawa and A. Kunugi, *Electrochem. Commun.*, **1**, 459 (1999).
15. Y. Yan, M. Zhang, K. Gong, L. Su, Z. Guo, and L. Mao, *Chem. Mater.*, **17**, 3457 (2005).
16. U. Yogeswaran and S. M. Chen, *Sens. Actuators B*, **130**, 739 (2008).
17. Y. W. Ju, G. R. Choi, H. R. Jung, and W. J. Lee, *Electrochim. Acta*, **53**, 5796 (2008).
18. C. Y. Du, T. S. Zhao, and Z. X. Liang, *J. Power Sources*, **176**, 9 (2008).
19. M. D. Rubianes and G. A. Rivas, *Electrochem. Commun.*, **9**, 480 (2007).
20. C. Y. Wang, V. Mottaghitalab, C. O. Too, G. M. Spinks, and G. G. Wallace, *J. Power Sources*, **163**, 1105 (2007).
21. X. L. Xie, Y. W. Mai, and X. P. Zhou, *Mater. Sci. Eng. R.*, **49**, 89 (2005).
22. M. M. Waje, X. Wang, W. Li, and Y. Yan, *Nanotechnology*, **16**, S395 (2005).
23. U. Yogeswaran, S. Thiagarajan, and S. M. Chen, *Anal. Biochem.*, **365**, 122 (2007).
24. E. Frackowiak, V. Khomenko, K. Jurewicz, K. Lota, and F. B'eguin, *J. Power Sources*, **153**, 413 (2006).
25. V. C. Dall'Orto, C. Danilowicz, S. Sobral, A. L. Balbo, and I. Rezzano, *Anal. Chim. Acta*, **336**, 195 (1996).
26. C. Paul-Roth, J. Rault-Berthelot, G. Simonneaux, C. Poriel, M. Abdalilah, and J. Letessier, *J. Electroanal. Chem.*, **597**, 19 (2006).
27. P. Schulthess, D. Ammann, W. Simon, C. Caderas, R. Stepanek, and B. Krautler, *Helv. Chim. Acta*, **67**, 1026 (1984).
28. D. Ammann, M. Huser, B. Krautler, B. Rusterholz, P. Schulthess, B. Lindemann, E. Halder, and W. Simon, *Helv. Chim. Acta*, **69**, 849 (1986).
29. A. Hodinar and A. Jyo, *Chem. Lett.*, **17**, 993 (1988).
30. M. Huser, W. E. Morf, K. Fluri, K. Seiler, P. Schulthess, and W. Simon, *Helv. Chim. Acta*, **73**, 1481 (1990).
31. N. A. Chaniotakis, A. M. Chasser, M. E. Meyerhoff, and J. T. Groves, *Anal. Chem.*, **60**, 185 (1988).
32. S. B. Park, W. Matuszewski, M. E. Meyerhoff, Y. H. Liu, and K. M. Kadish, *Electroanal. Chem.*, **3**, 909 (1991).
33. C. Shi and F. C. Anson, *Inorg. Chem.*, **29**, 4298 (1990).
34. E. Song, C. Shi, and F. C. Anson, *Langmuir*, **14**, 4315 (1998).
35. P. A. MacCarthy and A. M. Shah, *Coron. Artery Dis.*, **14**, 109 (2003).
36. R. Rodrigo and G. Rivera, *Free Radic Biol. Med.*, **33**, 409 (2002).
37. Y. Wang, J. Huang, C. Zhang, J. Wei, and X. Zhou, *Electroanal. Chem.*, **10**, 776 (1998).
38. W. B. Nowall and W. G. Kuhr, *Electroanal. Chem.*, **9**, 102 (1997).
39. D. P. Root, G. Pitz, and N. Priyantha, *Electrochim. Acta*, **36**, 855 (1991).
40. U. Yogeswaran and S. M. Chen, *Anal. Lett.*, **41**, 210 (2008).
41. S. M. Chen, Y. L. Chen, and R. Thangamuthu, *J. Solid State Electrochem.*, **11**, 1441 (2007).
42. S. M. Chen and M. I. Liu, *Electrochim. Acta*, **51**, 4744 (2006).
43. S. M. Chen, C. J. Liao, and V. S. Vasantha, *J. Electroanal. Chem.*, **589**, 15 (2006).
44. J. Wang, J. Dai, and T. Yarlagadda, *Langmuir*, **21**, 9 (2005).
45. M. Tahhan, V. T. Truong, G. M. Spinks, and G. Wallace, *Smart Mater. Struct.*, **12**, 626 (2003).
46. T. Komura, G. Y. Niu, T. Yamaguchi, M. Asano, and A. Matsuda, *Electroanal. Chem.*, **16**, 1791 (2004).
47. J. W. Shie, U. Yogeswaran, and S. M. Chen, *Talanta*, **74**, 1659 (2008).
48. C. P. Andrieux, O. Haas, and J. M. SavGant, *J. Am. Chem. Soc.*, **108**, 8175 (1986).